UNIVERSIDAD NACIONAL DE COLOMBIA
SEDE MEDELLÍN
FACULTAD DE MINAS

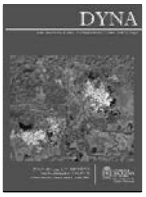

DYNA
http://dyna.medellin.unal.edu.co/

Analysis and stiffness evaluation of a microparallel kinematic machine

Ricardo Yañez-Valdez

Facultad de Ingeniería, Universidad Nacional Autónoma de México, México DF, México. ryv77@unam.mx

Received: November 16th, de 2016. Received in revised form: May 5th, 2017. Accepted: May 23th, 2017

Abstract
This study explores a scaled version of a 3-PRRR parallel configuration that can be used in micro-machining tasks. The study addresses a stiffness model of a micro-parallel kinematic machine (mPKM) by employing an approach involving kinematic and static equations. The objective of the model includes providing an understanding of the manner in which the stiffness of a mechanism changes as a function of both the position of an end-effector and the estimated cutting forces that are generated by micro-machining operations. An experimental prototype is considered for the preliminary validation. Three work planes and three cutting directions into the workspace are evaluated by iso-stiffness mapping. The results indicate that the mPKM operates with high stiffness performances in static operations. This is useful for suitable improvements in the prototype and developing analytical design criteria.

Keywords: Isotropic behavior; micromanufacturing; microparallel kinematic machine; set-up prototype; stiffness maps.

Análisis y evaluación de la rigidez de una micro máquina herramienta paralela

Resumen
Este trabajo explora una versión escalada de la configuración paralela 3PRRR para ser usada como micromáquina herramienta. Se propone una metodología para obtener mapas de rigidez mediante un modelo teórico y un prototipo experimental. El objetivo principal es definir un conjunto de directrices que permitan, a su vez, establecer criterios de diseño. Se presenta un modelo de rigidez basado en la teoría de trabajo virtual con el propósito de comprender como cambia la rigidez de la máquina en función de la posición del actuador final y las fuerzas de corte generadas por una operación de micromaquinado. Tres planos de trabajo y tres direcciones de corte han sido evaluados mediante mapas de rigidez. El resultado muestra que la micromáquina provee suficiente rigidez para realizar operaciones de micromaquinado.

Palabras clave: Isotropía de fuerzas; mapas de rigidez; mecanismo paralelo; micromanufactura; micromáquina herramienta.

1. Introduction

The demand for micro-devices (1–1,000 μm) is rapidly increasing to meet the growing needs in different fields such as biomedical and micro-electronic fields. This demand is in the form of new applications that require better performance, lower cost, and higher quality [1]. In Japan, a study proposed a new method to reduce the size of small part production equipment to a level that is comparable with the size of the parts produced for the purpose of generating significant savings with respect to energy, space required, and resources throughout a production plant [2]. The size of micromachine tools is defined by means of the ratio between the volume of a workspace and the volume of a machine. With respect to a micromachine, the overall volume of the machine is 125-1,000 times the size of its working volume [3].

Mechanical micromachining involves-scaled down versions of turning, milling, and drilling as a set of micro-manufacturing processes and is gaining significant importance because of the viability of producing 3D miniature functional parts [4-6]. The appearance of design requirements that include size and weight reductions for

How to cite: Yañez-Valdez, Y., Analysis and stiffness evaluation of a microparallel kinematic machine, DYNA 84(201), pp. 224-233, 2017.

© The author; licensee Universidad Nacional de Colombia.

individual pieces and entire assemblies has resulted in the investigation of micro-equipment technology fabrication, representing immense opportunity for future development [7-8]. Extant studies have verified the effects of miniaturization of production systems on energy savings and material resources [2].

In order to develop micromachining tasks, a tool is coupled to a mechanism with a topology that traditionally consists of an open-loop kinematic Cartesian-type structure. The performance (including maximum velocity, force transmission, accuracy, and stiffness) of a micromachine tool is strongly influenced by the type of kinematic structure, and thus the advantages of micromachining are closely related with those of serial topology. As expected, the kinematic description of this arrangement constitutes the simplest of all configurations. In an X-Y-Z configuration, the movement of a tool in any direction is linearly related to the movements of the axis of each actuator (decoupling). Therefore, the performance of this type of configuration is steady across the entire regular workspace [9]. With respect to the design of micromachine tools, the goal involves ensuring simplicity for manufacturing and assembly. Simplicity is key in reducing the time required for development because simplicity increases the viability of reusing similar mechanical elements in several different parts of the machine [10]. Additionally, an appropriate design can help in simplifying dynamic modeling, reducing computation time, and consequently allowing for higher operating velocities (higher machining speeds and feeds) due to reduced moving mass and dynamic response capability [11,12].

The presence of parallel configurations is steadily increasing with respect to conventional manufacturing tasks [13-15] (for e.g. Parallel Kinematic Machines (PKMs)), its application to micromachining tasks is less evident. A primary feature of parallel mechanisms corresponds to the mechanical structure that is formed by one or more closed-loop kinematic chains. The main advantage of parallel mechanisms relates to the structural stiffness caused by multiple connections to the ground. Hence, the load to weight ratio in parallel mechanisms exceeds those in serial mechanisms. For the same reason, given the same errors on individual joint variables, parallel mechanisms produce a lower positioning error when compared to those of serial mechanisms when input errors are assumed as the only sources of inaccuracy [16]. However, only practice (and not theory) indicates as to whether or not it is possible to manufacture parallel mechanisms with more accuracy than serial mechanisms [16]. The hypothesis is that parallel mechanisms are potentially better than the serial ones if an appropriate topology and optimum dimensions are selected for a specific task.

In most parallel mechanisms, a motion is coupled between the position and orientation of the end-effector. The workspace is not regular. This presents a high non-linear input-output relationship. Additionally, the Jacobian matrix that transforms the joint rates of mechanisms into an end-effector velocity state is not isotropic. Consequently, the performance varies considerably for different points in the Cartesian space and for different directions at a given point. This is in opposition to the requirements of the micromachining process in which isotropic behavior is required for each direction of the load. These requirements include a regular workspace, the capacity to transmit homogeneous force, a minimum variation in the stiffness values, and a low cost for the components and the control. Furthermore, a purely translational mobility is required to perform basic micromachining operations. Several 3-DOF (degrees of freedom) architectures were proposed by previous studies to achieve pure translational motions by using various theoretical approaches [17,18].

In micro-equipment applications, parallel mechanisms are regularly used as micro-manipulators [19,20] and micro-positioning platforms [21]. Recently, extant studies suggested the application of parallel mechanisms to micromachining tasks. For example, with respect to the energetic processes field, flexure-based micro-manipulators are increasingly common within the last decade. An EDM (Electrical Discharge Machining) micromachine uses a Delta configuration to manipulate an electrode [22]. However, most of the configurations involve coupled motion between the position and orientation of the end-effector. Thus, the inclusion of these types of configurations in micro-mechanical tasks could lead to unexpected performance results. Furthermore, it is difficult to design a decoupled parallel mechanism that possesses simultaneous translational and rotational movement [23].

Recent research on 3-DOF parallel mechanisms (conventional scale) lean towards decoupling of the position and orientation of an end-effector and the elimination of a complicated multi-DOF joint. Kim and Tsai [24] conceived a 3PRRR (active prismatic pair-passive revolute joints) parallel mechanism that which employs only revolute and prismatic joints to achieve pure translational motion of a moving platform and behaves in a menner similar to a traditional X–Y–Z Cartesian machine. Kong and Gosselin patented and analyzed a 3CRR (active cylindrical pair-passive revolute joints) Translational Parallel Mechanism (TPM, which is termed as Tripteron) that is similar to the Cartesian Parallel Mechanism (CPM) presented by Tsai [25,26]. Gosselin et al. discussed the design [27] and several properties [28] of the Tripteron that belongs to a multipteron family. Li et al. [29] presented the design of a new 3-DOF translational platform that employs only revolute joints. Yen and Lai [30] derived a dynamic model of a 3-DOF CPM for control purposes. The principle of inserting flexible elements into a 3PRRR mechanical structure was investigated in a previous study [31]. A conventional scale 3PRRR parallel configuration was extensively analyzed by extant research. However, it is not explored in the micro-mechanical field to date.

Stiffness analysis plays a significant role in designing PMs. Stiffness characteristic analysis is also an important research topic. In order to investigate the stiffness characteristics of PMs, a few studies proposed effective approaches for stiffness matrix decomposition [32-34]. An extant study presented a model by establishing a relationship between stiffness matrices of the platform and joint/links [35] in which the concept of a virtual joint was introduced to express bending and torsional compliance, and this result in a simplified model represented by two one-dimensional

lumped springs. Subsequently, this idea was widely used by other studies [12,36,37] and was significantly improved in a previous study [38-40] in which a multidimensional lumped-parameter model presents joints/links as pseudo-rigid with virtual springs. This approach led to the proposal of systematic methods for stiffness modeling of parallel mechanisms by combining screw theory with a virtual joint method [41].

Given the fore-mentioned reasons, the present study involved developing a 3-DOF microparallel kinematic machine (mPKM) based on a selection procedure. In the study, the features that allowed the mechanism to be feasible as a micromachine tool are evaluated, the stiffness model is addressed by means of a Jacobian matrix, a stiffness mapping methodology is set, its validation on the mPKM is demonstrated, and the most important conclusions are presented from the collected results.

2. Parallel configuration selection

Several possible ways exist to use basic joints to construct kinematic chains, and thus there are many possible parallel configurations. An appropriate parallel structure is dependent on the task to be completed. Based on the selection of a 3-DOF parallel mechanism, a 3PRRR parallel configuration was selected to design and build a mPKM prototype [42]. This proposal accounts for the essential advantages of serial open-loop configurations such as a regular workspace, homogeneous performance (constant velocity and force transmission ratios in the workspace), and decoupled geometry.

Fig. 1 shows a step-by-step design approach for the mechanism. The basic idea involves selecting a common 3-DOF parallel mechanism that inherits essential advantages from Cartesian micromachine tool configurations and developing a microparallel kinematic machine prototype.

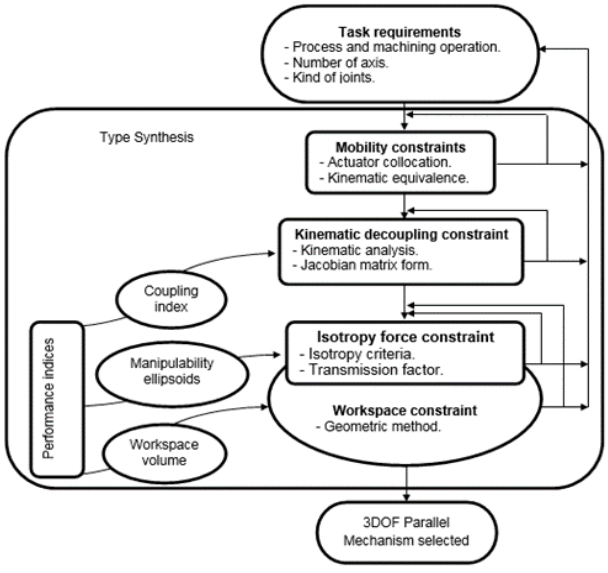

Figure 1. A step-by-step design approach for a 3-DOF PM [42]. Source: The authors.

Additionally, constraints are introduced mainly to satisfy functional requirements. Subsequently, the analysis of each constraint is quantitatively evaluated by using performance indices such as a coupling index, manipulability ellipsoids, and workspace volume.

The following section explains the development and characterization of the mPKM prototype.

3. Microparallel kinematic machine

3.1. Architecture description

The mechanical configuration of the mPKM is symmetric, and it is composed of three identical limbs (the X-, Y-, and Z-axes) that connect the fixed base to the end-effector triangle as shown in Fig. 2. The design of the mPKM based on the following requirements:

A. At least 3-DOF translational mobility in the linear stages.
B. Production of pieces ranging from 50 micrometers to a few millimeters.
C. Maximum workspace corresponding to 20 mm x 20 mm x 20 mm.
D. Minimum resolution corresponding to 1 μm.
E. Repeatability exceeding 10 μm.
F. A rapid traverse approximately corresponding to 150–200 mm/min.

Each limb comprises a PRRR design with three passive revolute joints and an active prismatic joint. The P joint is directly driven by a linear actuator assembled on the fixed base. The mechanism provides linear motion for each axis. From the kinematic analysis, a simple kinematic relation is expressed as follows:

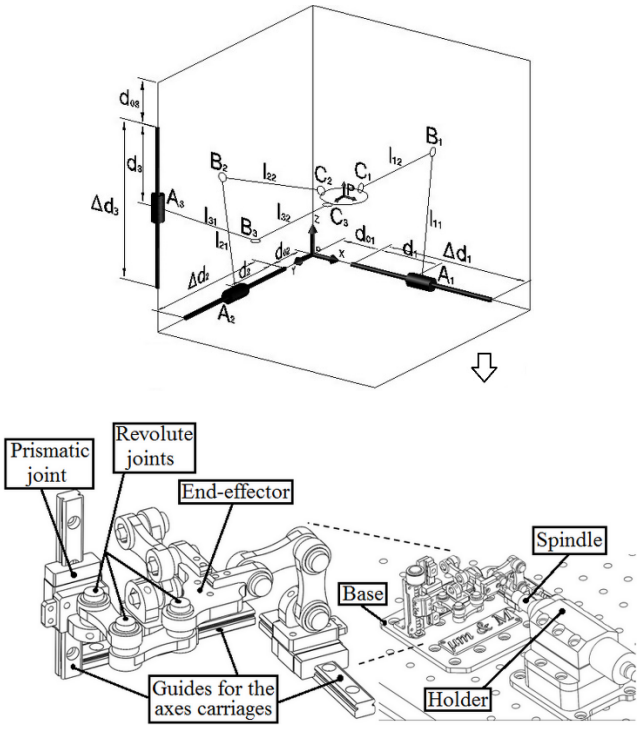

Figure 2. Sketch and Topology of the microparallel kinematic machine. Source: The authors.

$$\begin{bmatrix} P_x \\ P_y \\ P_z \end{bmatrix} = \begin{bmatrix} d_{01} + d_1 \\ d_{02} + d_2 \\ d_{03} + d_3 \end{bmatrix} \quad (1)$$

where P_x, P_y and P_z define the position of the coordinate frame *xyz*. The starting point of a prismatic joint is defined by d_i, and the sliding distance is defined by d_{0i}. The motion in each axis draws a linear trajectory, and this implies movement in one direction when only an actuator is activated. Additionally, the mechanical configuration shows a completely decoupled architecture. The orthogonal arrangement of the three linear actuators cause the configuration to provide a regular workspace in a parallelepiped form as shown in Fig. 3.

A one-to-one correspondence exists between the input and the output displacements, velocities and forces, and the mechanic configuration that is proven as isotropic across the entire workspace [42]. These conditions guarantee isotropic behavior in each direction of motion and nearly constant stiffness values.

3.2. Prototype assembly and description

Mechanical errors can be associated with the part, the machine, or the operation/process, and are introduced due to several reasons. Machine structural components and their orientation and relative motion are major contributors of mechanical errors [43]. The assembly of machine components into a machine results in their individual behavior contributing to the overall behavior of the machine. In this sense, the prototype is fabricated by designing only one axis and then duplicating the same to complete the machine. Additionally, the prototype is assembled carefully to avoid kinematic errors caused by misaligned components during assembly work. A detailed schematic of the prototype assembly process is shown in Fig. 4.

Additionally, each link of the micromachine includes an array as a cantilever mount. The cantilever joint involves two miniature bearings. A thrust bearing is used to bear the axial load. A baa bearing is used to handle the radial load and to reduce friction. The internal diameter of both bearings corresponds to 3 mm. A shoulder screw with a hardened shank serves as a pivot pin.

The dimensions of the machine correspond to 120 mm x 100 mm x 70 mm. The machine provides a workspace of 15 mm x 15 mm x 15 mm. As shown in Fig. 5, the mPKM is

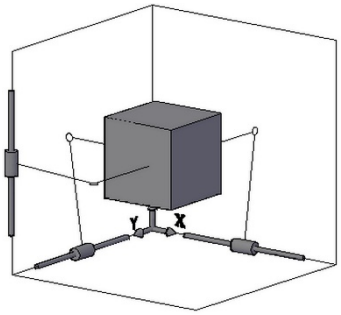

Figure 3. Reachable workspace of the 3PRRR TPM.
Source: The authors.

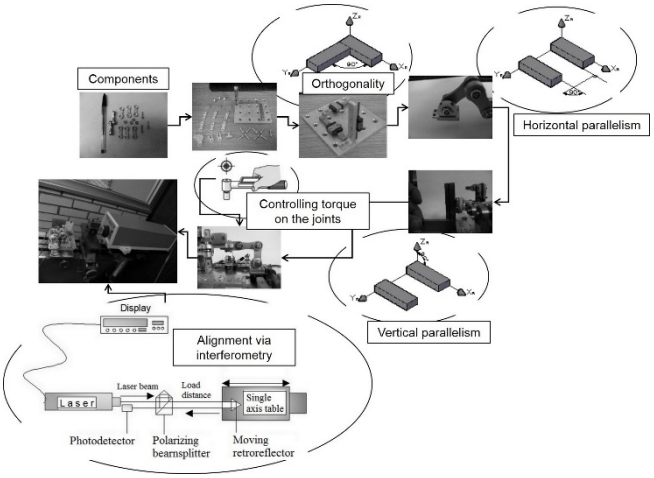

Figure 4. Assembly process of the prototype.
Source: The authors.

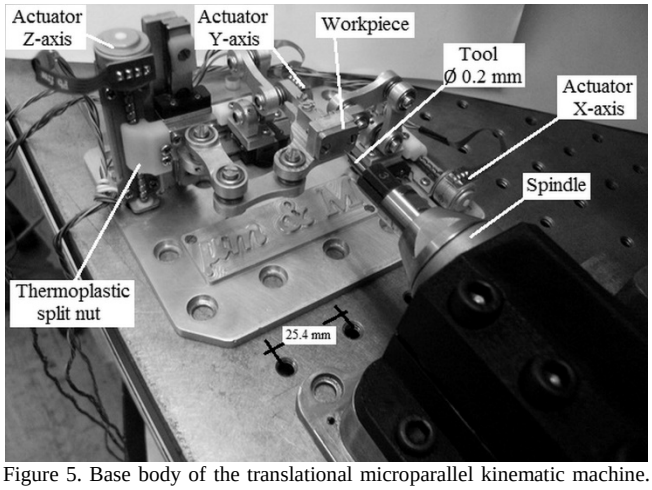

Figure 5. Base body of the translational microparallel kinematic machine.
Source: The authors.

composed of only a base body that is installed on a vibration isolation workstation. The spindle and the motion control correspond to independent systems. The majority of the components are aluminum. Each leg is connected at an end to the guide ways by means of ABS-grade lead split nuts.

3.3. Experimental evaluation of the suggested design approach

The displacements of the developed prototype along each axis are obtained with stepper motors that behave as actuators and are coupled to the limbs by means of a direct-drive transmission. These types of actuators are controlled by a three-axis stepper motor power driver that provides a micro-stepping mode to minimize the vibrations and positioning error. The theoretical resolution of each axis corresponds to 600 nm. The displacements for each axis of the mechanism are controlled by a PC-based control system by using a PCI-7340 board and a MID-7604/7602 power drive. With respect to the metrology process, a group of 1080 measurements for

Table 1.
Parameters of the feed system.

axis	Stroke range [mm]	Resolution [µm]	Repeatability [µm]	Standard deviations [mm]	Backlash average [µm]
X	15	0,6	4,1	0,003	6,5
Y	15	0,6	3,9	0,006	17,8
Z	15	0,6	3,4	0,009	12,3

Source: The authors.

each axis that is distributed across the entire workspace are considered and analyzed. The repeatability of the machine is evaluated by using a series of twenty bidirectional positioning moves over the entire stroke. The parameters including backlash are summarized in Table 1.

Tests are performed to evaluate the performance modeling as suggested in the design of the mPKM. The experimental tests focus on a simple evaluation of the characteristics for micro-manufacturing tasks as described in section 2.

Mobility: The prototype provides 3-DOF translational mobility by using linear stages. The motions are completely decoupled, i.e., they are performed independently. The stroke of each actuator corresponds to 15 mm with rapid traverse movements corresponding to 180 mm/min. Additionally, the ratio of the overall volume of the machine to the size of its working volume corresponds to 249, which verifies that the mPKM prototype constitutes a micromachine tool.

Uniformity of the distribution of the tool forces: This corresponds to the qualitative capability of the machine to apply forces in the directions of the cutting forces. These types of cutting forces combine tangential (F_t), feed (F_f), and radial (F_r) forces in an orthogonal approach. Hence, the uniformity of the distribution of the tool forces must be present in the fore-mentioned directions. A simple experimental test is conducted to experimentally prove this condition.

Each actuator is operated by means of the control system by covering the full stroke of the machine. This is achieved by placing the prototype in the vertical direction, and the effect of a constant external force (such as gravity) is considered acting in the negative direction for each axis. In turn, a set of precision weights is placed over the end-effector and proceeds gradually until movement becomes impossible. The highest value measured in each case is recorded. If the highest value recorded in limb 1 matches the value recorded in limb 2 and so forth, then the machine possesses the capability to uniformly provide forces. Furthermore, in order to analyze the sensitivity of the assembly under different adjustment conditions, the test is performed as follows:

Case a
- Aligned guide ways system.
- Joint torque range adjustment from 0.045 Nm to 0.050 Nm.
- Lead split nuts torque range adjustment from 0.02 Nm to 0.025 Nm.

Case b
- Aligned guide ways system.
- Joint torque uniform adjustment corresponding to 0.045 Nm.
- Lead split nuts uniform adjustment corresponding to 0.02 Nm.

In each case, the motor (20P step motor) parameters are as follows: velocity corresponding to 0.15 m/s, acceleration corresponding to 30 m/s^2, supply current corresponding to 0.5 A, and 40 steps/revolution. These were achieved by micro-stepping the stepper motor. In order to obtain torque control on the joints and the lead nuts, a digital programmable torque wrench ranging from 0.020 Nm to 4.0 Nm and a resolution of 0.001 Nm was used. The results of the experimental test are shown in Table 2.

Table 2 shows the experimentally measured forces in each direction of movement for the two different adjustment conditions. The results show that a non-uniform adjustment in the joints and the lead split nuts significantly influences the force transmission capabilities of the machine even in closed intervals of adjustment (i.e., with a difference not exceeding 0.005 Nm). However, each chain adjustment is uniform when the joint and the lead split nut adjustments possess the same torque. Therefore, the distribution of the tool forces in an orthogonal approach is uniform. In the following section, all subsequent analyses are performed by setting the machine as corresponding to case b.

4. Experimental stiffness

4.1. Basic Assumptions

In order to evaluate configuration stiffness, a virtual joint method based on a lump modeling approach is applied [24]. Based on this approach, the deflection between two members of a revolute joint is modeled as an infinitesimal rotation relative to an axis perpendicular to the axis of revolution. This deflection axis is termed as a virtual axis [24]. Therefore, it is feasible to consider each limb in conjunction with a moving platform as corresponding to a serial arm with three virtual axes as shown in Fig. 6.

Table 2.
Experimental data.

Axis	- Case a - Load capacity [kg]	Force [N]	Axis	- Case b - Load capacity [kg]	Force [N]
X	0,105	1,03	X	0,135	1,32
Y	0,088	0,86	Y	0,132	1,29
Z	0,075	0,73	Z	0,135	1,32

Source: The authors.

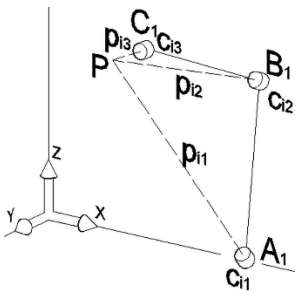

Figure 6. Isolate limb of the mPKM with three virtual compliant joints.
Source: The authors.

An expression relating the infinitesimal displacement of rotation with the forces acting in the end-effector is as follows:

$$\delta \mathbf{p} = C\mathbf{f} \tag{2}$$

Where $\delta \mathbf{p} = \left[\delta p_x, \delta p_y, \delta p_z\right]^T$, $\mathbf{f} = \left[f_x, f_y, f_z\right]^T$ and C denotes a diagonal compliance matrix whose diagonal elements are given by $C_{ij} = c_{i1}p_{i1}^2 + c_{i2}p_{i2}^2 + c_{i3}p_{i3}^2$. Where, c_{ij} denotes an angular compliance constant, and $p_{ij} = \left\| p_{ij} \right\|$ denotes the distance between a virtual axis of compliance and the end-effector, *P*. Writing Eq. (1) three times, once for each limb, i = 1, 2 and 3, yields:

$$\begin{aligned} \delta p_x &= \left(c_{11}p_{11}^2 + c_{12}p_{12}^2 + c_{13}p_{13}^2\right) f_x \\ \delta p_y &= \left(c_{21}p_{21}^2 + c_{22}p_{22}^2 + c_{23}p_{23}^2\right) f_y \\ \delta p_z &= \left(c_{31}p_{31}^2 + c_{32}p_{32}^2 + c_{33}p_{33}^2\right) f_z \end{aligned} \tag{3}$$

Therefore, we obtain the stiffness mapping as:

$$\mathbf{f} = \mathbf{K}\delta\mathbf{p} \tag{4}$$

Where ***K***, the stiffness matrix of the mechanism in the Cartesian space, is then given by following expression:

$$\mathbf{K} = k\mathbf{J}^T\mathbf{J} \tag{5}$$

with

$$k = \begin{bmatrix} 1/k_1 & 0 & 0 \\ 0 & 1/k_2 & 0 \\ 0 & 0 & 1/k_3 \end{bmatrix}$$

Therefore, it is necessary to compute corresponding reference points since the matrix **K** varies with respect to the workspace. This analysis produces stiffness maps that describe the end-effector compliance as a function of the mechanism configuration [44,45].

4.2. Experimental procedure

The specifications and the cutting forces present in a basic micro-machining process are shown in Table 3. It is generated based on the relationship between the mechanical properties of work materials and the cutting condition, a cutter tool diameter corresponding to 0.2 mm, and an optimal cutting speed for the implemented spindle. All the cutting conditions are proposed based on practical knowledge.

Three work planes are selected to represent the cutting force components inside the workspace of the mPKM. Each work plane in turn represents three different positions and elevations of the moving platform as shown in Fig. 7. This is due to the operational concept in which the spindle is placed horizontally to facilitate its alignment.

Table 3.
Specifications and cutting forces of micro machining milling process.

	Specification					Cutting forces		
Material	S_{ut} [MPa]	Tϕ [mm]	SS [r.p.m.]	Lf [mm/min]	Dc [mm]	F_t	F_f	F_r
Al (6061-T6)	200	0,2	36.000	100	0,03	3	1	0,7
BR (272)	300					6	2	1
SST (AISI 304)	480					19	9	4
Ti (Ti6Al4V)	900					31	21	12

S_{ut} Ultimate tensile strength. Tϕ Tool diameter. SS Spindle speed. Lf Linear feed. Dc Depth of cut. F_t Tangential force in mN. F_f Feed force in mN. F_r radial force in mN.
Source: The authors.

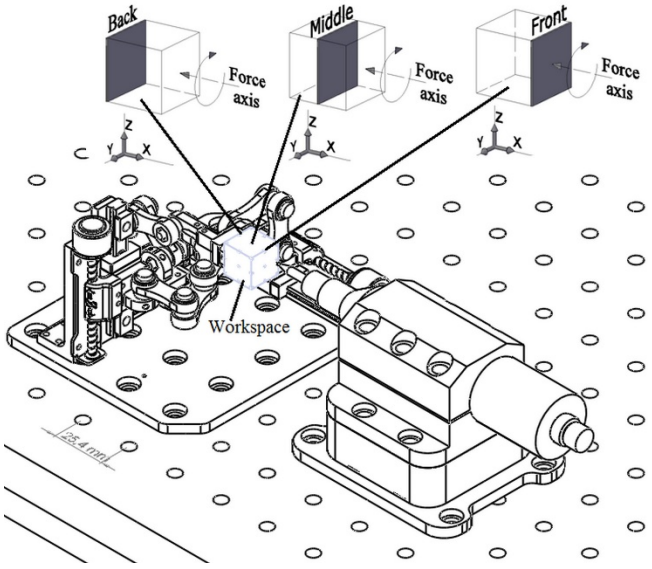

Figure 7. Three geometric work planes inside workspace. Back (x = 15 mm), middle (x = 7,5 mm), and front (x = 0 mm).
Source: The authors.

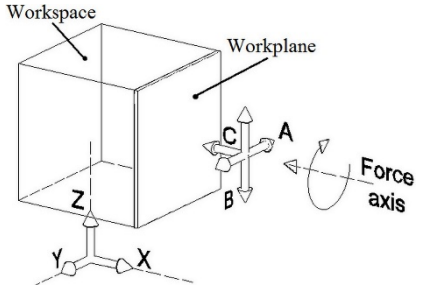

Figure 8. A) Horizontal direction parallel to Y-axis; B) Vertical direction parallel to Z-axis; and C) Depth direction parallel to X-axis.
Source: The authors.

With respect to the stiffness that must be provided to the machine, attention must focus mainly in three directions as shown in Fig. 8.

Fig. 9 depicts the experimental prototype, equipment used in the experimental measurements, and masses used for load application.

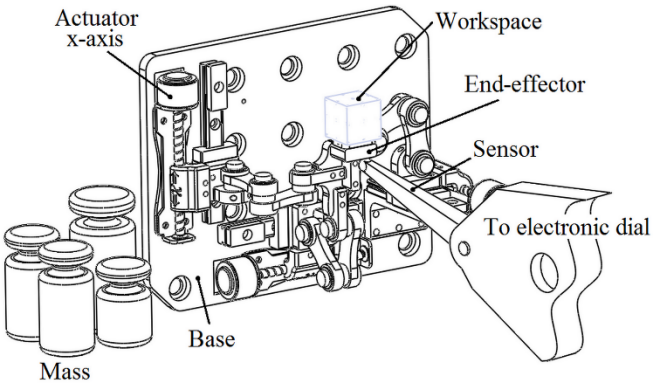

Figure 9. Schematic diagram: experimental measurement setup.
Source: The authors.

The procedure for the experimental stiffness analysis includes the following steps. A representative number of measurements are defined after the manipulator workspace is known. The measurements are placed in three different positions and elevations on the moving platform for each axis. The current position to be measured is fixed by means of the control system or by manual placement. This condition determines the starting localization of the moving platform during the experiment. A preload is applied to the system to eliminate gaps and manufacturing errors. These errors are introduced due to tolerances and adjustments in the manufacturing process and the assembly of the prototype. Finally, the value of the total displacement is obtained by gradually increasing the load and providing realistic measurements that represent the resistant behavior of the prototype.

4.3. Experimental stiffness measurement

An experimental procedure is described for obtaining the mPKM stiffness within its workspace. Subsequently, the methodology for measurements is implemented based on characteristics of the mPKM prototype.

The **K** stiffness is obtained with the measurement devices in the experimental method. This data provides information with respect to the stiffness of the mPKM prototype when the load is applied in the vertical direction. Therefore, the prototype is placed in the vertical position. As shown in Fig. 9, the instrumentation for the experimental measurements includes a dial indicator with a resolution of 0.1 µm. The laboratory test conditions approximately corresponded to 50% humidity with a temperature of 21 °C.

The measurement position of the prototype is established by means of manual placement. Subsequently, the installation of the measuring devices is set, and each of the experimental tests is completed by following the protocol detailed in this section. The experimental measurements are collected in three work planes in the workspace for a total of 27 measurements as shown in Fig. 10. The mPKM prototype includes three translational DOF, and thus it is only possible to represent the variations in a parameter. Thus, the stiffness for a constant orientation is evaluated.

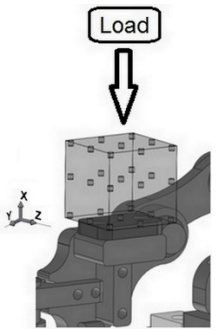

Figure 10. Measured points in the workspace.
Source: The authors.

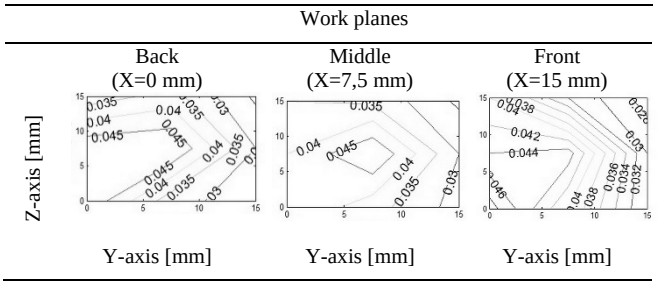

Figure 11. Contour stiffness maps for the experimental measurements, [N/µm].
Source: The authors.

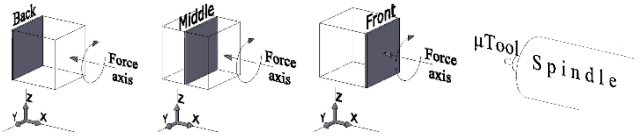

Figure 12. Three geometric work planes inside the workspace.
Source: The authors.

A few design parameters are proposed to analyze the localization effect of the actuators. The parameters include link length l_{i1}=l_{i2}=20 mm, end-effector radius r=15 mm, actuators travel Δd_i=15 mm, and an estimated angular compliant constant corresponding to C_{ij}=0,015 rad/mNm. The parameters define a workspace corresponding to 15 mm x 15 mm x 15 mm. Three identical work planes (Fig. 7) are selected to represent the contour maps inside the workspace.

The **K** map for the three work planes is obtained from the experimental results as shown in Fig. 11. The work planes correspond to those shown in Fig. 12. This is due to the operational concept during the machining process in which a spindle is placed horizontally to facilitate its alignment.

The experimental model presents the maximum values away from the X-axis while the minimum values are along the center work plane. Table 4 compares the average measured stiffness in each work plane. The simulation values shown in Table 4 are calculated by considering the real dimensions of the prototype and the virtual joint method.

Table 4.
Comparison of the stiffness.

Work plane	Stiffness average	
	Simulation data [N/μm]	Experimental data [N/μm]
Back	0,041	0,036
Middle	0,037	0,035
Front	0,035	0,037

Source: The authors.

Table 5.
Summary of displacements into the mPKM workspace [μm].

	Direction								
	Back			*Middle*			*Front*		
Material	δ_x	δ_y	δ_z	δ_x	δ_y	δ_z	δ_x	δ_y	δ_z
Al (6061-T6)	0,01	0,05	0,01	0,01	0,05	0,01	0,01	0,06	0,01
BR (272)	0,03	0,10	0,01	0,03	0,11	0,01	0,03	0,12	0,02
SST (AISI 304)	0,17	0,33	0,07	0,17	0,36	0,06	0,17	0,39	0,08
Ti (Ti6Al4V)	0,40	0,55	0,21	0,40	0,59	0,18	0,40	0,64	0,25

Source: The authors.

Additionally, the load capacity of the mPKM is measured. A load of 20 g is supported without producing significant displacement of the end-effector by using the same experimental setup and applying a torque of 0.045 Nm in the joints of the prototype. This is verified for three identical work planes.

5. Results and discussion

The present study highlighted the most interesting features of a 3PRRR parallel configuration including the kinematics, workspace, and static stiffness. Eq. (1) shows that both the inverse and direct kinematics of the mechanism are independent of link lengths. Therefore, the TPM is insensitive to errors in the link lengths. Theoretically, although these types of errors affect the coordinates of the passive revolute joints, they do not affect the position of the moving platform. In practice, the errors present in the joints are transmitted to the end-effector and cause systematic errors such as hysteresis. However, it is possible to avoid the negative effect transmitted to the end-effector by applying a homogeneous torque during the assembly of the joints.

The cutting forces in a micro machining milling process are considered to establish a relationship between forces and displacements. The magnitude of the resulting displacement δ due to cutting force is determined based on Eq. (6) in the linear range.

$$k = \frac{f_c}{\delta} \tag{6}$$

where f_c and k denote the magnitude of the cutting force component acting on the workpiece and the elements of the stiffness into each work plane, respectively. Table 5 shows the summary of results.

The results indicate that the primary source of compliance is provided for the joints. The bearings in the revolute joints possess moment loads perpendicular to their axis of rotation and limit the achievable stiffness of the machine. However, the obtained stiffness maps represent a useful tool for the end user of the micromachine. With respect to a given set of spatial coordinates, the stiffness maps allow accurate selection of workspace zones that are most suitable for the stiffness requirements. Additionally, the range of forces that can be withstood by the end-effector without suffering deformation are in the order of 0.19 N.

With respect to the same force range that can be provided by the end-effector, larger components of force are susceptible to exceed the force of the end-effector, and this is especially true if the cut depth is increased. Therefore, it is necessary to increase the stiffness of the micromachine to address this vulnerability. This is possible because the stiffness of the machine is dependent on the stiffness of the joint, and thus an increase in the torque present in the joints leads to increased stiffness in the micromachine. Fig. 13A shows the torque-range in the joints and the force resulting in the critical zone in which a lower stiffness is present. However, this possibility involves a demand for greater torque to the actuators. An increase in the required torque increases the size of the actuator. It should be noted that the selected actuators can be larger in comparison to the mechanical structure because scaling laws are not compatible with miniaturization and especially in the case of electro-mechanical devices [46], such as motors. However, they are highly dynamic and possess sufficient torque to drive a parallel structure in a direct-drive configuration. This condition does not constitute a disadvantage because a possibility of fixing the actuators on the mechanism of a frame exists. Fig. 13B shows the torque demand on the actuators when the torque-range in the joints increases.

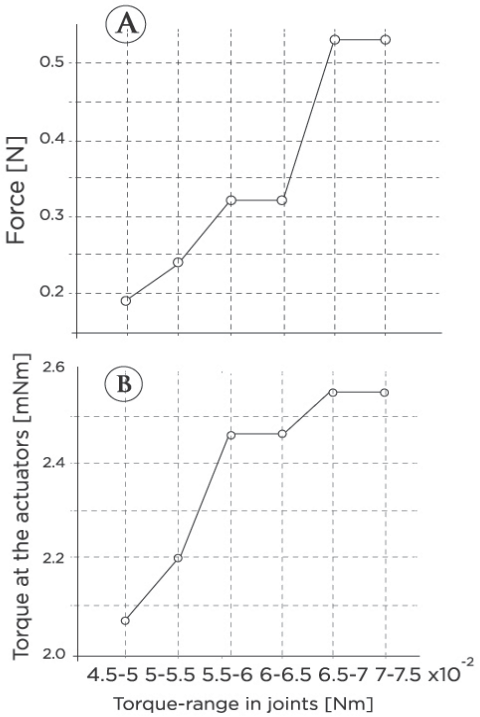

Figure 13. Torque-range in the joints versus A) minimal force in the moving platform, and B) torque at the actuators demanded.
Source: The authors.

Finally, a necessary condition for a micromachine to withstand external loads relates to the stiffness of the structural parts exceeding the stiffness of the external body. This assumes that the micro-scale dynamic load is negligible due to the low inertia of the moving parts that causes small dynamic actions with respect to the strength of the structural material. This consideration implies that scaling down a thinner section is sufficiently strong to withstand external actions such as limbs that constitute a parallel arrangement.

6. Conclusions

The present study describes the design of a mechanical architecture for micromachining applications. This configuration corresponds to a translational parallel mechanism that behaves in a manner similar to a conventional X-Y-Z Cartesian machine. The 3-DOF TPM provides sufficient mobility to perform basic micromachining tasks. The results indicate that the kinematic and static properties are significant mainly due to the Cartesian arrangement of the structure that grants a decoupling of the motion. The results reveal that the mechanism offers conditions that can guarantee isotropic behavior for each load direction. In order to practically validate the requirements, a microparallel kinematic machine based on the 3-PRRR parallel mechanism is designed and constructed. Performance tests are conducted to examine the feasibility of the micromachining process. The performance tests indicate that the system can perform micromachining tasks. Future studies will incorporate manufacturing task strategies, such as 2D and 3D micro-milling, to test machining capability.

Acknowledgments

Thanks to Centre for Applied Science and Technological Development at UNAM for the opportunity to develop this project supported by DGEP UNAM.

References

[1] Dornfeld, D., Min, S. and Takeuchi, Y., Recent advances in mechanical micromachining, manufacturing technology. Annals of the CIRP, 55(2), pp. 745-768. 2006. DOI: 10.1016/j.cirp.2006.10.006

[2] Kawahara, N., Suto, T., Hirano, T., Ishikawa, Y., Kitahara, T., Ooyama, N. and Ataka, T., Microfactories, new applications for micromachine technology to the manufacture of small products, Microsystem Technologies, 2(2), pp. 37-41, 1997. DOI: 10.1007/s005420050052

[3] Ehmann, K.F., DeVor, R.E., Kapoor, S.G. and Cao, J., Design and analysis of Micro/Meso-scale machine tools, in Smart Devices and Machines for Advanced Manufacturing, Wang, L. and Xi, J., (Eds.), Springer, pp. 283-318, 2008.

[4] Chae, J., Park, S. and Freiheit, T., Investigation of micro cutting operations. International Journal of Machine Tools and Manufacture, 46(3-4), pp. 313-332, 2006. DOI: 10.1016/j.ijmachtools.2005.05.015

[5] Masuzawa, T., State of the art of micromachining. CIRP Annals-Manufacturing Technology, 49(2), pp. 473-488, 2000. DOI: 10.1016/S0007-8506(07)63451-9

[6] Dhanorker, A. and Ozel, T., Meso-micro scale milling for micro manufacturing. International Journal in Mechatronics and Manufacturing Systems, 1(1), pp. 23-42, 2008. DOI: 10.1504/IJMMS.2008.018273

[7] Dario, P., Valleggi, R., Carrozza, M.C., Montesit, M.C. and Coccot, M., Microactuators for microrobots: A critical survey. Journal in Micromechanics and Microengineering, 2(3), pp. 141-157, 1999. DOI: 10.1088/0960-1317/2/3/005

[8] Fujita, H., Microactuators and micromachines, in Proc. of the IEEE (invited paper), 86(8), pp. 1721-1732, 1998. DOI: 10.1109/5.704278

[9] Yoshikawa, T., Manipulability and redundant control of mechanisms, in Proc. of the IEEE, Int. Conf. Robotics and Automation, 2, pp. 1004-1009, 1985. DOI: 10.1109/ROBOT.1985.1087283

[10] Ruiz-Huerta, L., Caballero-Ruiz, A. and Kussul, E., Guide lines for low cost micromechanics in Aspe XVII Annual Meeting, St. Louis, Missouri, pp. 228-233, 2002.

[11] Xie, F., Liu,X.-J., Analysis of the kinematic characteristics of a high-speed parallel root with Schönflies motion: Mobility, kinematics, and singularity. Frontiers of Mechanical Engineering, 11(2), pp. 135-143, 2016. DOI:10.1007/s11465-016-0389-7

[12] Zhang, D. and Wang, L., Conceptual development of an enhanced tripod mechanism for machine tool. Robotics and Computer-Integrated Manufacturing, 21(4-5), pp. 318-327, 2005. DOI: 10.1016/j.rcim.2004.11.010.

[13] Wang, Y., Zou, H., Zhao, Y. and Li, M., Design and kinematics of a parallel manipulator for manufacturing. Annals of the CIRP-Manufacturing Technology, 46(1), pp. 297-300, 1997. DOI: 10.1016/S0007-8506(07)60829-4

[14] Kanaan, D., Wenger, P. and Chablat, D., Kinematic analysis of a serial-parallel machine tool: The Verne machine. Mechanism and Machine Theory, 44(2), pp. 487-498, 2009. DOI: 10.1016/j.mechmachtheory.2008.03.002

[15] Wenger, P. and Chablat, D., Kinematic analysis of a new parallel machine tool: The orthoglide, in Advances in Robot Kinematics, Lenarnic, J. and Stanisic, M.L., (Eds.), Kluwer Academic Publishers, London, pp. 305-314, 2000. DOI: 10.1007/978-94-011-4120-8_32

[16] Briot, S. and Bonev, I., Are parallel robots more accurate than serial robots?. Transactions of the Canadian Society for Mechanical Engineering, 31, pp. 445-455, 2007.

[17] Carricato, M. and Parenti-Castelli, V., A Family of 3-DOF translational parallel manipulators. Journal of Mechanical Design, 125(2), pp. 302-307, 2003. DOI: 10.1115/1.1563635

[18] Li, Y. and Xu, Q., Kinematic analysis and design of a new 3-DOF translational parallel manipulator. Journal of Mechanical Design, 128(4), pp. 729-737, 2006. DOI: 10.1115/1.2198254

[19] Heikkilä, H.R., Karjalainen, I.T., Uusitalo, J.J., Vuola, A.S. and Tuokko, R.O., Possibilities of a microfactory in the assembly of small part and products-first result of the M4-project, in Proceedings of the 2007 International Symposium on Assembly and Manufacturing, Ann Arbor, Michigan, USA, pp. 166-171, 2007.

[20] Perroud, S., Codourey, A. and Mussard, Y., A Miniature robot for the microfactory. CSEM Centre Suisse d'Electronique et de Microtechnique, Switzerland, 2003.

[21] Kang, D.S., Seo, T.W., Yoon, Y.H., Shin, B.S., Liu, X-J. and Kim, J., A micro positioning parallel mechanism platform with 100 degree tilting capability. Annals of the CIRP Manufacturing Technology, 55(1), pp. 377-380, 2006. DOI: 10.1016/S0007-8506(07)60439-9

[22] Beltrami, I., Joseph, C., Clavel, R., Bacher, J.P. and Bottinelli, S., Micro-and nanoelectric-discharge machining. Journal of Materials Processing Technology, Elsevier, 149(s 1-3), pp. 263-265, 2004. DOI: 10.1016/j.jmatprotec.2004.03.002

[23] Zhang, J.J., Li, W.M., Wang, X.H. and Gao, F., Study on kinematics decoupling for parallel manipulator with perpendicular structures, in Proceedings of the 2006 IEEE/RSJ International Conference on Intelligent Robots and Systems, Beijing, China, pp. 748-753, 2006. DOI: 10.1109/IROS.2006.282624

[24] Kim, H.S. and Tsai, L.W., Design optimization of a Cartesian parallel manipulator. Journal of Mechanical Design, 125(1), pp. 43-51, 2003. DOI: 0 10.1115/1.1543977

[25] Kong, X. and Gosselin, C.M., Kinematics and singularity analysis of a novel type of 3-CRR 3-DOF translational parallel manipulator. The International Journal of Robotics Research, 21(9), pp. 791-798, 2002. DOI: 10.1177/027836490202100905O1

[26] Gosselin, C.M., Kong, X., Cartesian Parallel Manipulators, US Patent No. 6,729,202 B2 May 4, 2004.

[27] Gosselin, C., Kong, X., Foucault, S. and Bonev, I., A fully-decoupled 3-DOF translational parallel mechanism, in Proc. 4th Chemnitz Parallel Kinematics Seminar (PKS), pp. 595-610, 2004.
[28] Gosselin, C.M., Masouleh, M.T., Duchaine, V., Richard, P-L., Foucault, S. and Kong, X., Parallel mechanisms of the multipteron family: Kinematic architectures and benchmarking, in International Conference on Robotics and Automation, Roma, Italy, 10-14 April 2007. DOI: 10.1109/ROBOT.2007.363045
[29] Li, W., Gao, F. and Zhang, J., A three-DOF translational manipulator with decoupled geometry. Robotica, 23(6), pp. 805-808, 2005. DOI: 10.1017/S0263574705001700
[30] Yen, P.L. and Lai, C-C., Dynamic modeling and control of a 3-DOF Cartesian parallel manipulator. Mechatronics, 19(3), pp. 390-398, 2009. DOI: 10.1017/S0263574705001670
[31] Bruzzone, L. and Molfino, R., A novel parallel robot for current microassembly applications in Assembly Automation, 26(4), pp. 299-306, 2006. DOI: 10.1108/01445150610705218
[32] Loncaric, J., Normal forms of stiffness and compliance matrices. IEEE Journal on Robotics and Automation, 3(6) pp. 567-572, 1987. DOI: 10.1109/JRA.1987.1087148
[33] Huang, S. and Schimmels, J.M., The eigenscrew decomposition of spatial stiffness matrices. IEEE Transactions on Robotics and Automation, 16(2), pp. 146-156, 2000. DOI: 10.1109/70.843170
[34] Chen, G., Wang, H., Lin, Z. and Lai, X., The principal axes decomposition of spatial stiffness matrices. IEEE Transactions on Robotics, 31(1), pp. 191-207, 2015. DOI: 10.1109/TRO.2015.2389415
[35] Zhang, D. and Gosselin, C.M., Kinetostatic modeling of N-DOF parallel mechanisms with a passive constraining leg and prismatic actuators. Journal of Mechanical Design, 123(3) pp. 375-381, 2000. DOI:10.1115/1.1370976
[36] Zhang, D., Xi, F., Mechefske, C.M. and Lang, S.Y.T., Analysis of parallel kinematic machine with kinetostatic modelling method. Robotics and Computer-Integrated Manufacturing, 20(2), pp. 151-165, 2004. DOI: org/10.1016/j.rcim.2003.08.005
[37] Zhang, D., Bi, Z. and Li, B., Design and kinetostatic analysis of a new parallel manipulator. Robotics and Computer-Integrated Manufacturing, 25(4-5), pp. 782-791, 2009. DOI: 10.1016/j.rcim.2008.10.002
[38] Pashkevich, A., Chablat, D. and Wenger, P., Stiffness analysis of overconstrained parallel manipulators. Mechanism and Machine Theory, 44(5), pp. 966-982, 2009. DOI: 10.1016/j.mechmachtheory.2008.05.017
[39] Pashkevich, A., Klimchik, A. and Chablat, D., Enhanced stiffness modeling of manipulators with passive joints. Mechanism and Machine Theory, 46(5), pp. 662-679, 2011. DOI: https://doi.org/10.1016/j.mechmachtheory.2010.12.008
[40] Klimchik, A., Pashkevich, A., Caro, S. and Chablat, D., Stiffness matrix of manipulators with passive joints: Computational aspects. IEEE Transactions on Robotics, 28(4), pp. 955-958, 2012. DOI: 10.1109/TRO.2012.2187395
[41] Liu, H., Huang, T., Chetwynd, D.G. and Kecskeméthy, A., Stiffness modeling of parallel mechanisms at limb and joint/link levels. IEEE Transactions on Robotics, 99, pp. 1-8, 2017. DOI: 10.1109/TRO.2017.2654499
[42] Yañez-Valdez, R., Basis for the development of micro-parallel kinematic machines (in Spanish). Revista Iberoamericana de Automática e Informática Industrial RIAI, 11(2), pp. 212-223, 2014. DOI: 10.1016/j.riai.2014.02.004
[43] Dornfeld, D. and Dae-Eun, L., Precision Manufacturing Science+Business Media, LLC, Springer, 2008. DOI: 10.1007/978-0-387-68208-2
[44] Xi, F., Zhang, D., Mechefske, C.M. and Lang, S., Global kinetostatic modelling of tripod-based parallel kinematic machine. Mechanism and Machine Theory, 39(4), pp. 357-377, 2004.DOI: 10.1016/j.mechmachtheory.2003.09.007
[45] Gosselin, C., Stiffness mapping for parallel manipulator. IEEE Transactions on Robotics and Automation, 6(3), pp. 377-382, 1990. DOI: 10.1109/70.56657
[46] Kussul, E., Baidyk, T., Ruiz-Huerta, L., Caballero-Ruiz, A. and Velasco, G., Scaling down of microequipment parameters. Precision Engineering, 30(2), pp. 211-222, 2006. DOI: 10.1016/j.precisioneng.2005.08.001

R. Yañez-Valdez, received the BSc. Eng in Industrial Engineering in 2002, the MSc. degree in Mechanical Engineering in 2007, and the PhD degree in Mechanical Engineering in 2012, the last one from the Universidad Nacional Autónoma de México (UNAM), Mexico. Currently, he is an associated professor in the Department of Mechanical Engineering, Facultad de Ingeniería at UNAM, Mexico. His research areas include: mechanism creation, and design, performance evaluation and enhancement, micromechanics and micromachining equipment design (more precisely applied to planar and spatial parallel mechanisms), as well as multibody dynamic and vibration modeling.
ORCID: 0000-0002-8518-0906.

UNIVERSIDAD NACIONAL DE COLOMBIA
SEDE MEDELLÍN
FACULTAD DE MINAS

Área Curricular de Ingeniería Mecánica

Oferta de Posgrados

Maestría en Ingeniería - Ingeniería Mecánica

Mayor información:

E-mail: acmecanica_med@unal.edu.co
Teléfono: (57-4) 4259262